COMPUTATIONAL COMPARISON BETWEEN THE TAYLOR–HOOD AND THE CONFORMING CROUZEIX–RAVIART ELEMENT

ROLF KRAHL [*] AND EBERHARD BÄNSCH[†]

Abstract. This paper is concerned with the *computational* performance of the P_2P_1 Taylor–Hood element and the conforming $P_2^+P_{-1}$ Crouzeix–Raviart element in the finite element discretization of the incompressible Navier–Stokes equations. To this end various kinds of discretization errors are computed as well as the behavior of two different preconditioners to solve the arising systems are studied.

Key words. Taylor–Hood element, Crouzeix–Raviart element, incompressible fluid flow, preconditioners for Quasi-Stokes

AMS subject classifications. 65N30, 76M10

1. Introduction. In [11] Taylor and Hood proposed the $Q_2^{(8)}Q_1$ element on quadrilaterals for solving the Navier–Stokes equations numerically. This is a variant of the biquadratic-bilinear Q_2Q_1 element, but with the central node in the velocity space removed. Since then, it became common practice to refer to the Q_2Q_1 element on quadrilaterals as well as to its triangular counterpart, the P_2P_1 element, both in 2D and in 3D, as "Taylor–Hood element". This combination of finite element spaces has become one of the most well-known and popular elements for solving the incompressible Navier–Stokes equations.

In [7] Crouzeix and Raviart analyzed a further class of finite element spaces on triangular meshes for the Stokes equations, of which at least two became also rather popular in CFD and are referred to as "Crouzeix–Raviart element" nowadays: the non-conforming P_1P_0 element, where the velocity is continuous at the midpoints of the element faces only, see e.g. [1, 12], and the conforming $P_2^+P_{-1}$ element, see e.g. [2, 8, 10].

Much effort has been spent to analyze various classes of elements. However, there are significantly less *computational* investigations to compare different types of element regarding their actual discretization errors and computational performance in general. The aim of this article is to present *some* computational results in order to provide some rationale for assessing the behavior and performance of the P_2P_1 and the conforming $P_2^+P_{-1}$ elements. This paper summarizes results from [13].

The rest of this paper is organized as follows: in Section 2 we present the numerical problem we are concerned with, introduce some notations, and define the preconditioners tested in this paper. In Section 3 we recall the definition of the Taylor–Hood and the conforming Crouzeix–Raviart element. This is followed by Section 4, where the performance of both elements is tested in various ways. Preconditioners for the Quasi-Stokes problem are the objective of Section 5.

[*]Weierstraß-Institut für Angewandte Analysis und Stochastik, Mohrenstraße 39, 10117 Berlin, Germany, `krahl@wias-berlin.de`

[†]Friedrich-Alexander-Universität Erlangen-Nürnberg, Lehrstuhl für Angewandte Mathematik III, Haberstraße 2, 91058 Erlangen, Germany, `baensch@mi.uni-erlangen.de`

2. Numerical methods. We are concerned with the numerical solution of the instationary, incompressible Navier–Stokes equations in a bounded domain $\Omega \subset \mathbf{R}^d$, $d \in \{2, 3\}$ and some time interval $\mathbf{T} \subset \mathbf{R}_+$: for a given right hand side $\mathbf{f}$, Dirichlet boundary data $\mathbf{u}_D$ and initial function $\mathbf{u}_0$ find a pair $(\mathbf{u}, p)$ of a velocity and pressure field fulfilling

$$
\begin{aligned}
\partial_t \mathbf{u} + \mathbf{u} \cdot \nabla \mathbf{u} - \frac{1}{Re} \Delta \mathbf{u} + \nabla p &= \mathbf{f} & &\text{in } \mathbf{T} \times \Omega, \\
\nabla \cdot \mathbf{u} &= 0 & &\text{in } \mathbf{T} \times \Omega, \\
\mathbf{u} &= \mathbf{u}_D & &\text{on } \mathbf{T} \times \partial\Omega, \\
\mathbf{u} &= \mathbf{u}_0 & &\text{in } \{0\} \times \Omega
\end{aligned}
\tag{2.1}
$$

with Re the Reynolds number. In order to determine the pressure uniquely, as usual we impose the condition $\int_\Omega p = 0$.

The structure of the solver used in this paper for the computational solution of (2.1) is described in [3]. It uses algorithms proposed in [5]. The following simplified "Quasi-Stokes" problem appears as a core subproblem after the time discretization: find $(\mathbf{u}, p)$ such that

$$
\begin{aligned}
\mu \mathbf{u} - \nu \Delta \mathbf{u} + \nabla p &= \mathbf{f} & &\text{in } \Omega, \\
\nabla \cdot \mathbf{u} &= 0 & &\text{in } \Omega, \\
\mathbf{u} &= \mathbf{u}_D & &\text{on } \partial\Omega
\end{aligned}
\tag{2.2}
$$

for certain parameters $\mu, \nu > 0$. Since the Quasi-Stokes problem is linear, we fix $\mu = 1$ hereafter.

Let us remark that in a more general situation the core problem to be solved in each time step may be an Oseen equation and thus being nonlinear. In this case the setting is computationally less convenient, since it prohibits the use of CG methods. Other Krylov space methods might be used instead.

2.1. Schur complement formulation of the Quasi-Stokes problem. The weak formulation of (2.2) is written in the usual form: find $(\mathbf{u}, p) \in \mathbf{u}_D + X \times Y$ such that

$$
\begin{aligned}
a(\mathbf{u}, \boldsymbol{\varphi}) + b(\boldsymbol{\varphi}, p) &= \langle l, \boldsymbol{\varphi} \rangle & &\forall \boldsymbol{\varphi} \in X, \\
b(\mathbf{u}, \psi) &= 0 & &\forall \psi \in Y
\end{aligned}
\tag{2.3}
$$

where X and Y are appropriate function spaces for the velocity and the pressure and a, b, and l are defined as

$$
a : X \times X \to \mathbf{R}, \quad a(\mathbf{u}, \mathbf{v}) = \mu \int_\Omega \mathbf{u} \cdot \mathbf{v} + \nu \int_\Omega \nabla \mathbf{u} : \nabla \mathbf{v},
$$

$$
b : X \times Y \to \mathbf{R}, \quad b(\mathbf{v}, p) = - \int_\Omega p \, \nabla \cdot \mathbf{v},
$$

$$
l \in X', \quad \langle l, \mathbf{v} \rangle = \int_\Omega \mathbf{f} \cdot \mathbf{v}.
$$

Using operators $A : X \to X'$, $B : X \to Y'$, and $B^T : Y \to X'$ defined as

$$
\langle A\mathbf{u}, \mathbf{v} \rangle = a(\mathbf{u}, \mathbf{v}), \qquad \langle B\mathbf{u}, q \rangle = b(\mathbf{u}, q), \qquad \langle B^T p, \mathbf{v} \rangle = b(\mathbf{v}, p)
$$

$\forall \mathbf{u}, \mathbf{v} \in X, \forall p, q \in Y$, problem (2.3) can be written as: find $(\mathbf{u}, p) \in X \times Y$ such that

$$
\begin{aligned}
A\mathbf{u} + B^T p &= l, \\
B\mathbf{u} &= 0.
\end{aligned}
\tag{2.4}
$$

Note that in this paper for ease of presentation we shall use the notation A, B, B^T also for matrices representing discretized versions of these operators. The meaning will be clear from the context.

Now this problem is equivalent to the *Schur complement formulation*: find $p \in Y$ such that

$$
BA^{-1}B^T p = BA^{-1}l \qquad \text{and} \qquad \mathbf{u} = A^{-1}(l - B^T p).
\tag{2.5}
$$

In this paper we consider solvers based on this Schur complement formulation. Preconditioned CG methods are used to solve (2.5). Preconditioning of the Schur complement operator is crucial, since the Schur complement operator degenerates for $\frac{\mu}{\nu} \to \infty$. The specific choices of preconditioners are addressed in the following section.

2.2. Preconditioners for the Quasi-Stokes problem. In this section we introduce two different preconditioners for the Schur complement formulation (2.5). The first one (called *Laplace preconditioner* hereafter) follows PDE ideas, while the second one is based on the discretized equations (*mass diagonal preconditioner*).

2.2.1. Laplace preconditioner. In [5] Bristeau, Glowinski, and Periaux proposed a preconditioner for the Quasi-Stokes problem (2.5) based on the solution of a Laplace problem in the pressure space: for a given $p \in Y$ let q be the solution of

$$
\begin{aligned}
-\Delta q &= p & &\text{in } \Omega, \\
\partial_\mathbf{n} q &= 0 & &\text{on } \partial\Omega.
\end{aligned}
\tag{2.6}
$$

Now set

$$
S_{Lp}^{-1} p := \mu q + \nu p.
\tag{2.7}
$$

We denote by $C_{Lp} = \left(\int_\Omega \nabla\psi_i \cdot \nabla\psi_j \right)$ the stiffness matrix in the pressure space. Then (2.6) can be written as $q = C_{Lp}^{-1}p$. Ol'shanskii proved in [14] that in fact this preconditioner is equal to the inverse of the Schur complement operator of the Quasi-Stokes problem for a particular set of model boundary conditions. Note that S_{Lp} becomes identity if $\mu = 0$ and $\nu = 1$.

The Laplace preconditioner has proven to perform very well with the Taylor–Hood element in practice with more realistic boundary conditions as for instance of Dirichlet type, which is also confirmed by our tests. However, for discontinuous pressure functions, it is not straightforward how to formulate and implement this preconditioner, since the Laplace operator requires H^1-regularity of the underlying space.

2.2.2. Mass diagonal preconditioner. As an alternative, we tested a preconditioner based on ideas presented in [15]. To this end we observe that the Quasi-Stokes problem does not need any preconditioning if $\frac{\mu}{\nu}$ is small. Therefore it is sensible to first consider the case $\frac{\nu}{\mu} \ll 1$. In this case we have

$$
\frac{1}{\mu}A = M + \frac{\nu}{\mu}D \approx M
\tag{2.8}
$$

with $M = \left(\int_\Omega \boldsymbol{\varphi}_i \cdot \boldsymbol{\varphi}_j \right)$ the mass matrix and $D = \left(\int_\Omega \nabla \boldsymbol{\varphi}_i : \nabla \boldsymbol{\varphi}_j \right)$ the stiffness matrix in the velocity space. Since M^{-1} is dense, we replace the mass matrix by its spectrally equivalent diagonal part $\tilde{M} = (\delta_{ij} M_{ij})$. The discrete Schur complement operator $BA^{-1}B^T$ is then approximated by $B\tilde{M}^{-1}B^T$.

To cover the full parameter range of μ and ν, we set

$$S_{MD}^{-1} p := \mu (B\tilde{M}^{-1}B^T)^{-1}p + \nu p. \tag{2.9}$$

Note that the matrix $C_{MD} = B\tilde{M}^{-1}B^T$ is computable, however the stencil is larger than for the usual Laplace's operator. The incidence matrix involves also neighbors of neighboring nodes of a vertex, see [4, 13] for details.

This mass diagonal preconditioner shows reasonable performance in practice, although not as good as the Laplace preconditioner for the Taylor–Hood element, see Section 5. Its main advantage is that it is based on the *matrices* of the saddle point problem only and does not introduce additional requirements on the regularity of the finite element spaces.

3. The Taylor–Hood and the Crouzeix–Raviart element. In this section, we recall the definition of the P_2P_1 Taylor–Hood and the $P_2^+P_{-1}$ conforming Crouzeix–Raviart finite element spaces.

First we need to fix some notations: assume for simplicity Ω to be polygonally shaped. Let $\mathcal{T}_h$ be a triangulation of Ω consisting of simplices. We assume the usual admissibility and shape regularity conditions on $\mathcal{T}_h$, see e.g. [6, Sec. 2.1–2.2].

For any $k \in \mathbf{N}$ and any simplex $S \subset \mathbf{R}^d$ we denote by

$$P_k(S) := \{ p : S \to \mathbf{R} \mid p \text{ is a polynomial of degree } \le k \}. \tag{3.1}$$

The P_2P_1 Taylor–Hood element consists of globally continuous, piecewise quadratic functions in the velocity space and of globally continuous, piecewise linear functions in the pressure space:

$$\begin{aligned} X_h^{TH} &:= \{ \mathbf{u} \in (C^0(\overline{\Omega}))^d \mid \forall S \in \mathcal{T}_h : \mathbf{u}_{|S} \in (P_2(S))^d \} \cap (H_0^1(\Omega))^d, \\ Y_h^{TH} &:= \{ p \in C^0(\overline{\Omega}) \mid \forall S \in \mathcal{T}_h : p_{|S} \in P_1(S) \} \cap L_0^2(\Omega). \end{aligned} \tag{3.2}$$

According to for instance [9] this combination of elements is LBB-stable, provided a rather general assumption on the triangulation is fulfilled.

In the case of the $P_2^+P_{-1}$ conforming Crouzeix–Raviart element, the pressure space consists of piecewise linear, *discontinuous* functions. The additional degrees of freedom must be balanced by enriching the velocity space by e.g. *volume bubbles* Φ_v and *face bubbles* Φ_f for the LBB-condition to hold. More precisely, let

$$\Phi_v(S) := \text{span}\left\{ \prod_{i=0}^d \lambda_i \right\} \quad \text{and} \quad \Phi_f(S) := \text{span}\left\{ \prod_{\substack{i=0 \\ i \neq k}}^d \lambda_i \mid k \in \{0, \dots, d\} \right\} \tag{3.3}$$

where λ_i are the barycentric coordinate functions with respect to S. Define

$$\begin{aligned} P_2^+(S) &:= P_2(S) \oplus \Phi_v(S) && \text{in 2D}, \\ P_2^+(S) &:= P_2(S) \oplus \Phi_v(S) \oplus \Phi_f(S) && \text{in 3D}. \end{aligned} \tag{3.4}$$

Level	Elements	DOF TH		DOF CR	
		X_h^{TH}	Y_h^{TH}	X_h^{CR}	Y_h^{CR}
1	8	50	9	66	24
2	32	162	25	226	96
3	128	578	81	834	384
4	512	2178	289	3202	1536
5	2048	8450	1089	12546	6144
6	8192	33282	4225	49666	24576

TABLE 4.1

Uniform refinement of the unit square in 2D. Number of degrees of freedom (DOF) for the Taylor–Hood and the conforming Crouzeix–Raviart element in the velocity and the pressure space.

Note that in 2D we have $\Phi_f(S) \subset P_2(S)$. Now define the $P_2^+ P_{-1}$ element by

$$
\begin{aligned}
X_h^{CR} &:= \{\mathbf{u} \in (C^0(\overline{\Omega}))^d \mid \forall S \in \mathcal{T}_h : \mathbf{u}_{|S} \in (P_2^+(S))^d\} \cap (H_0^1(\Omega))^d, \\
Y_h^{CR} &:= \{p \in L^2(\Omega) \mid \forall S \in \mathcal{T}_h : p_{|S} \in P_1(S)\} \cap L_0^2(\Omega).
\end{aligned}
\tag{3.5}
$$

Again, the proof of LBB-stability for this element can be found in in [9] (actually, there the proof is given for a variant with a slightly smaller velocity space; the LBB-stability for the $P_2^+ P_{-1}$ element as defined here, is a trivial corollary of this).

One main advantage of the discontinuous pressure functions of conforming Crouzeix–Raviart element is that the elementwise mean values of the divergence of discrete solutions $\mathbf{u}_h$ are zero and thus the discrete solutions fulfill a *local mass balance*. This is stated in the following theorem, which is readily proved.

THEOREM 3.1. *Let* $(\mathbf{u}_h, p_h) \in X_h^{CR} \times Y_h^{CR}$ *be the solution of the discrete Quasi-Stokes equations. Then we have for all* $S \in \mathcal{T}_h$:

$$
\int_S \nabla \cdot \mathbf{u}_h = 0.
\tag{3.6}
$$

4. Comparison of discretization errors. In this section we compare the Taylor–Hood and the conforming Crouzeix–Raviart element with respect to discretization errors. We start by studying the Quasi-Stokes problem (2.2), for which an analytic solution is available and thus the error can be computed exactly, see Section 4.1. Next we consider the full Navier–Stokes equations. There we first consider the dynamic behavior of the discrete solution for an instationary convection, see Section 4.2. Finally, we compare the two elements regarding the error in $\nabla \cdot \mathbf{u}_h$, see Section 4.3. We have run numerical experiments in 2D and in 3D. Since the results in 3D exhibit the same picture as the 2D examples, they are omitted here for sake of brevity.

Let us start by commenting on the triangulation. To keep things as concise as possible, we consider a uniform subdivision of the square in 2D and the cube in 3D. As for any given triangulation the function spaces X_h^{CR} and Y_h^{CR} are supersets of X_h^{TH} and Y_h^{TH} respectively, it is clear that the number of degrees of freedom for the conforming Crouzeix–Raviart element is higher than for the Taylor–Hood element. This increase is much more pronounced in the pressure space due to the discontinuities than in the velocity space. The number of degrees of freedom for a uniform refinement of a square in 2D are shown in Table 4.1.

Another indicator for the computational effort is the number of non-zero entries of the matrices involved. Table 4.2 shows the maximum number of non-zeros per

Matrix	2D		3D	
	TH	CR	TH	CR
A	25	33	125	293
B	50	14	375	45
B^T	9	24	27	192
C_{MD}	25	45	125	404
C_{Lp}	9	—	27	—

TABLE 4.2

Uniform refinement of the unit square in 2D and of the unit cube in 3D. Maximum number of non-zero entries per line in the matrices A, B, B^T, C_{MD}, and C_{Lp} for the Taylor–Hood and the conforming Crouzeix–Raviart element.

line for the matrices A, B, and B^T from the Quasi-Stokes problem (2.4) and for the matrices C_{Lp} and C_{MD} needed in the preconditioners as defined in Section 2.2.

4.1. Quasi-Stokes problem with known solution. The functions

$$\mathbf{u}(x,y) := \begin{pmatrix} \cos\left(\frac{\pi}{2}(x+y)\right) \\ -\cos\left(\frac{\pi}{2}(x+y)\right) \end{pmatrix}, \qquad p(x,y) := \sin\left(\frac{\pi}{2}(x-y)\right) \qquad (4.1)$$

are solution of the Quasi-Stokes system (2.2) in 2D with a suitable right hand side. When (2.2) is related to one time step of the time discretized Navier–Stokes equations (2.1), the parameter ν is proportional to $\Delta t/Re$, Δt the time step size, since μ was fixed to $\mu = 1$. Thus in practice, ν would be rather small. Therefore, in this section we study the discretization error $\mathbf{u} - \mathbf{u}_h$ and $p - p_h$ with respect to variations of ν ranging from $\nu = 10^{-6}$ to $\nu = 10^{-2}$.

This error is shown with respect to the number of degrees of freedom (DOF) in Figure 4.1. Clearly, for moderate values of ν the *experimental order of convergence* (EOC) approaches the expected values of 2 for the velocity and pressure in the H^1 and L^2-norms, respectively, and 3 for the velocity in the L^2-norm. Quantitatively, for given DOF the error in the pressure behaves very similarly for the Crouzeix–Raviart and the Taylor–Hood element. Concerning the velocity, the error is better by some factor for the Crouzeix–Raviart element compared to the Taylor–Hood element.

Only for the smallest value of $\nu = 10^{-6}$ the error curves for the velocity are not yet "saturated". However, the pressure behaves well also in this case.

4.2. Instationary convection. In order to test both elements with respect to the dynamic behavior of the instationary Navier–Stokes equations, we chose the example of an oscillating Bénard convection, compare also [3]. To this end the Navier–Stokes system (2.1) is augmented by a heat equation.

The examples has been solved in the unit square on very coarse grids in order to test the minimum level of grid refinement required to reproduce the oscillation. On a grid of refinement level 3 for the Taylor–Hood element and of level 2 for the Crouzeix–Raviart element, the expected oscillating pattern was visible, but heavily disturbed by other interrupting flow patterns. On even coarser grids the solver did not converge at all. On finer grids the oscillation was qualitatively well reproduced.

In a frequency analysis the results for the Crouzeix–Raviart element on a given level of grid refinement turn out to be similar to those from the Taylor–Hood element on a grid that is one level finer.

4.3. Comparison of $\nabla \cdot \mathbf{u}_h$. As already mentioned, one virtue of the Crouzeix–Raviart element is the local mass balance. Going a step further, in this section we
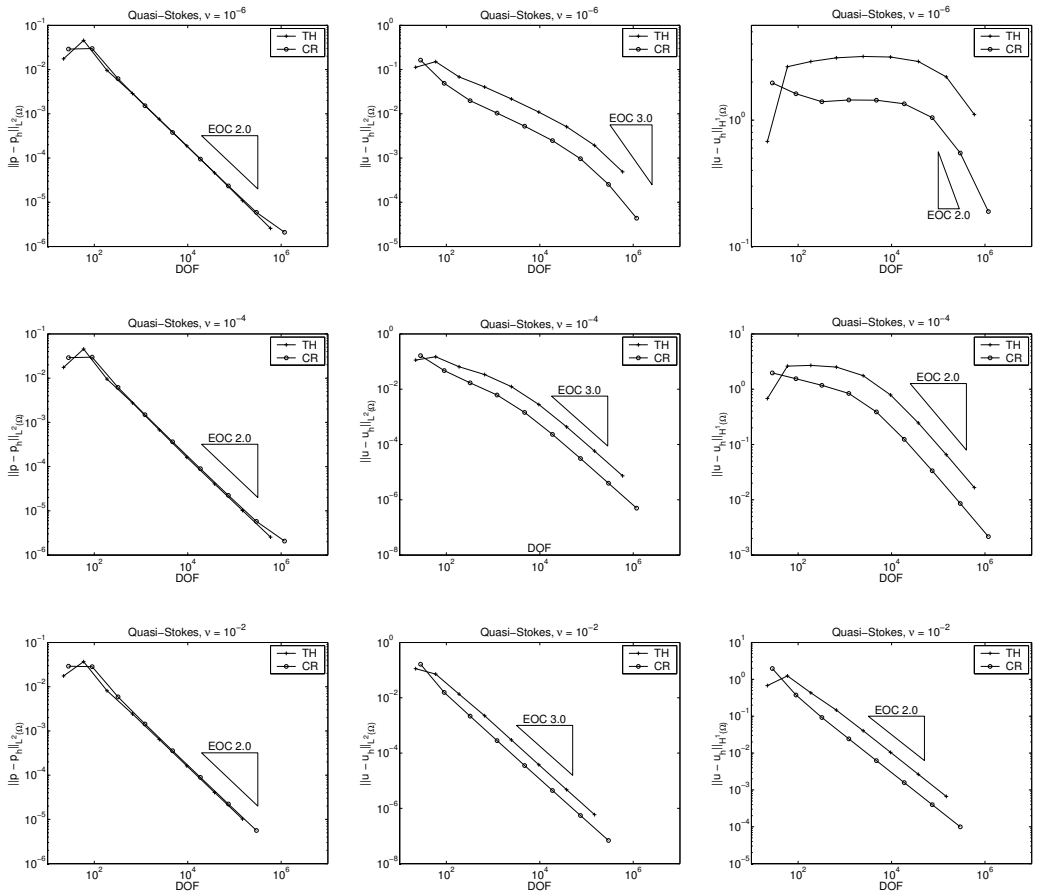
FIGURE 4.1. *Quasi-Stokes problem with $\mu = 1$ and $\nu = 10^{-6}$ (top), $\nu = 10^{-4}$ (center), and $\nu = 10^{-2}$ (bottom) for a known exact solution $(\mathbf{u}, p) \in X \times Y$. Discretization error $\|p - p_h\|_{L^2(\Omega)}$ (left), $\|\mathbf{u} - \mathbf{u}_h\|_{L^2(\Omega)}$ (center), and $\|\mathbf{u} - \mathbf{u}_h\|_{H^1(\Omega)}$ (right) vs. number of degrees of freedom.*

compare the two elements concerning the pointwise solenoidal condition. To this end, we first study an example with a smooth solution, a stationary Bénard convection in the unit square.

The results are shown in Figure 4.2. There, the error in $\nabla \cdot \mathbf{u}_h$ is measured in the L^2 as well as in the L^8-norm and plotted as a function of DOF. The reason for choosing the L^8-norm is that on one hand computationally an L^p-norm, $1 \leq p < \infty$, is much simpler to compute for higher order elements than the L^∞-norm and on the other hand for examples like this one the L^8-norm is rather close to the L^∞-norm.

As can be seen from the figures, the EOC takes on the expected value of 2 for both norms. Somewhat surprisingly, the error vs. DOF ratio is quite close for the Crouzeix–Raviart and the Taylor–Hood element.

The next example is the backward facing step. This example admits a singular solution due to the reentrant step. Therefore one cannot expect the full order of convergence. As shown in Figure 4.3 the EOC is of order 0.5 for $\nabla \cdot \mathbf{u}_h$ in the L^2-norm for both elements. Moreover, also as expected, there is divergence of $\nabla \cdot \mathbf{u}_h$ in the L^8-norm, somewhat stronger for the Taylor–Hood element. In this case of a
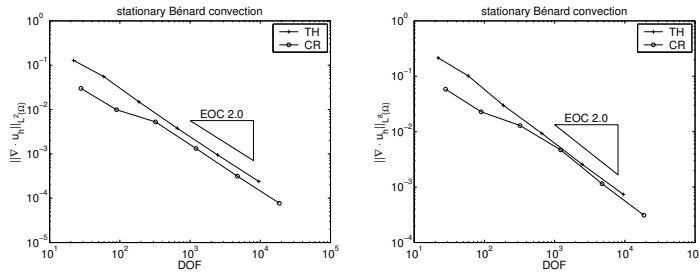
FIGURE 4.2. *Stationary Bénard convection. Behavior of $\nabla \cdot \mathbf{u}_h$ vs. number of degrees of freedom in the L^2-norm (left) and in the L^8-norm (right).*
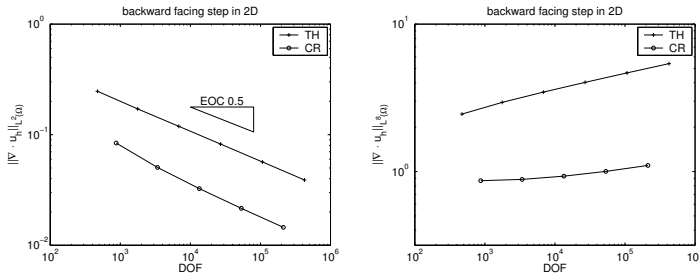

FIGURE 4.3. *Backward facing step in 2D. Behavior of $\nabla \cdot \mathbf{u}_h$ vs. number of degrees of freedom in the L^2-norm (left) and in the L^8-norm (right).*

singular solution the performance of the Crouzeix–Raviart element with respect to the solenoidal condition is much better than the Taylor–Hood element.

5. Comparison of preconditioners for the Quasi-Stokes problem. In order to test the performance of different preconditioners, we compare the number of iterations needed to solve the Quasi-Stokes problem. The following preconditioners have been tested:

No precond.:

$$S^{-1}p := p.$$

Laplace precond.: see Section 2.2.

$$S^{-1}p := \mu C_{Lp}^{-1}p + \nu p.$$

This preconditioner was used for the Taylor–Hood element only.

Mass diagonal precond.: see Section 2.2.

$$S^{-1}p := \mu(B\tilde{M}^{-1}B^T)^{-1}p + \nu p.$$

Plain mass diagonal precond.: The matrix of the mass diagonal preconditioner was used without adaptation to the parameters μ and ν of the problem.

$$S^{-1}p := (B\tilde{M}^{-1}B^T)^{-1}p$$

This preconditioner is only considered in order to demonstrate the difference of using $(B\tilde{M}^{-1}B^T)^{-1}$ compared to the linear combination $\mu(B\tilde{M}^{-1}B^T)^{-1} + \nu I$. Otherwise this preconditioner is of no practical use.
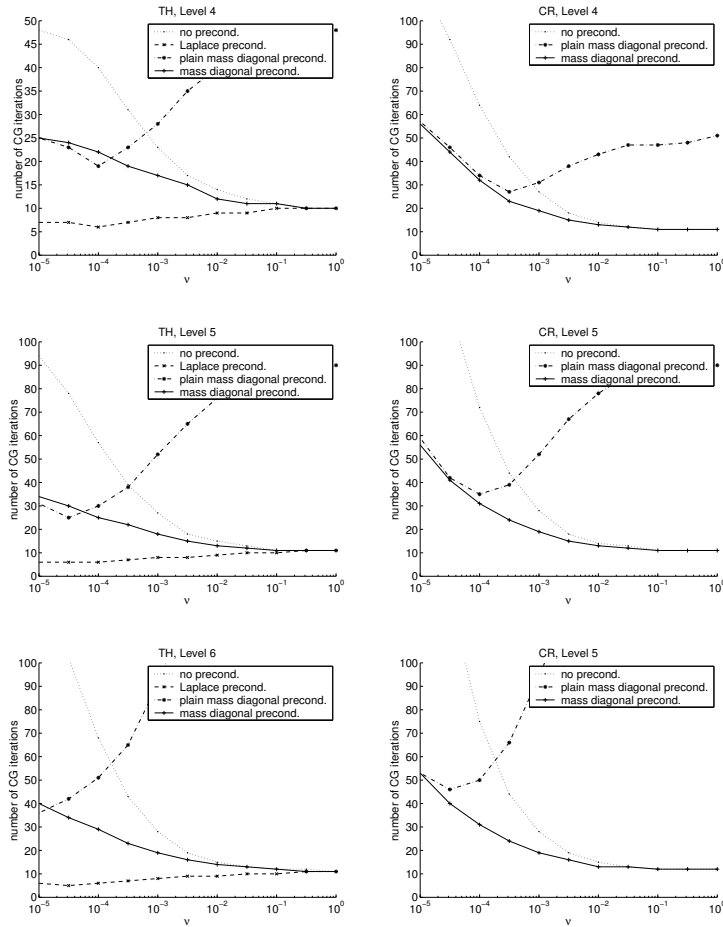
FIGURE 5.1. *Quasi-Stokes problem in 2D; $\mu = 1$. Number of iterations vs. ν using different preconditioners for the Taylor–Hood (left) and the conforming Crouzeix–Raviart element (right). Level of refinement 4 (top) to 6 (bottom).*

Figure 5.1 shows the number of iterations needed to solve the Quasi-Stokes problem in the Schur complement formulation (2.5) with a Conjugate Gradient method for a given tolerance. The parameter μ was fixed as $\mu = 1$ and ν was varied in the range $10^{-6} \le \nu \le 10^{0}$. The Taylor–Hood and the conforming Crouzeix–Raviart element was tested with different levels of refinement of the triangulation. Again we note that the same behavior can be observed in 3D. The corresponding figures are omitted for the sake of brevity.

As expected, our tests confirm the theoretical result that the Schur complement does not need preconditioning for large values of ν. For $\nu = 1$ both, the Laplace and the mass diagonal preconditioner, do not show any visible effect compared to no preconditioning. On the other hand, the Laplace preconditioner is also robust in terms of number of iterations over the whole range of values of ν. It performs even better for smaller values of ν. The mass diagonal preconditioner is able to keep the number of iterations within an acceptable range in most situations, but it still got problems with very small values of ν. It does not reach the performance of the Laplace

preconditioner.

6. Conclusions. The goal of this paper was a comparison of the computational performance of the Taylor–Hood and the conforming Crouzeix–Raviart element in the finite element discretization of the Navier–Stokes equations.

As one should expect from the additional number of degrees of freedom, the computational results for the Crouzeix–Raviart element are better in all tests than those from the Taylor–Hood element on the same grid. But also the costs in terms of computation time are higher. As a quite rough rule of thumb one can say, the results from the Crouzeix–Raviart element are by one level of grid refinement better, but they are also by one level of grid refinement more expensive than the results from the Taylor–Hood element. There is one major exception to this rule: for non-smooth solutions we observe that the the local mass balance, measured in terms of the pointwise solenoidal function, is much better fulfilled for the Crouzeix–Raviart than for the Taylor–Hood element.

Different preconditioners for the Quasi-Stokes problem have been compared. The Laplace preconditioner turns out to perform best in the whole parameter range. The fact that this preconditioner is not (directly) available for the Crouzeix–Raviart element is one important reason for the higher computational costs of this element resulting from our computational approach. We note, however, that this picture may change, if one would use static condensation to reduce the degrees of freedom for the Crouzeix–Raviart element or certain multigrid methods, which may be computationally cheaper for the Crouzeix–Raviart element than for the Taylor–Hood element.

REFERENCES

[1] T. APEL, S. NICAISE, AND J. SCHÖBERL, *A non-conforming finite element method with anisotropic mesh grading for the Stokes problem in domains with edges*, IMA J. Num. Anal., 21 (2001), pp. 843–856.
[2] F. H. BERTRAND, M. R. GADBOIS, AND P. A. TANGUY, *Tetrahedral elements for fluid flow*, Int. J. Numer. Methods Eng., 33 (1992), pp. 1251–1267.
[3] E. BÄNSCH, *Simulation of instationary, incompressible flows*, Acta Math. Univ. Comenianae, 67 (1998), pp. 101–114.
[4] E. BÄNSCH AND B. HÖHN, *Numerical treatment of the Navier–Stokes equations with slip boudary condition*, SIAM J. Sci. Comput., 21 (2000), pp. 2144–2162.
[5] M. O. BRISTEAU, R. GLOWINSKI, AND J. PERIAUX, *Numerical methods for the Navier–Stokes equations. applications to the simulation of compressible and incompressible viscous flow*, Comput. Phys. Reports, 6 (1987), pp. 73–187.
[6] P. G. CIARLET, *The Finite Element Method for Elliptic Problems*, North–Holland, Amsterdam, 1978.
[7] M. CROUZEIX AND P.-A. RAVIART, *Conforming and nonconforming finite element methods for solving the stationary Stokes equations*, R.A.I.R.O. R3, 7 (1973), pp. 33–76.
[8] C. CUVELIER, A. SEGAL, AND A. A. VAN STEENHOVEN, *Finite Element Methods and Navier–Stokes Equations*, Reidel, Dordrecht, 1986.
[9] V. GIRAULT AND P.-A. RAVIART, *Finite Element Methods for Navier–Stokes Equations*, Springer, 1986.
[10] P. M. GRESHO AND R. L. SANI, *Isothermal Laminar Flow*, volume 2 of *Incompressible Flow and the Finite Element Method*, 3rd edition, Wiley, Chichester, 2000.
[11] P. HOOD AND C. TAYLOR, *Navier–Stokes equations using mixed interpolation*, in *Finite Element Methods in Flow Problems*, J. T. ODEN, R. H. GALLAGHER, O. C. ZIENKIEWICZ, AND C. TAYLOR, eds., University of Alabama in Huntsville Press, 1974, pp. 121–132.
[12] P. KNOBLOCH AND L. TOBISKA, *The P_1^{mod} element: a new nonconforming finite element for convection-diffusion problems*, SIAM J. Numer. Anal., 41 (2003), pp. 436–456.
[13] R. KRAHL, *Das Crouzeix–Raviart–Element bei der numerischen Lösung der Navier–Stokes–Gleichung mit FEM*, Diplomarbeit, Universität Bremen, Studiengang Mathematik, 2002.

[14] M. OL'SHANSKII, *On the Stokes problem with model boundary conditions*, Sbornik: Mathematics, 188 (1997), pp. 603–620.

[15] S. TUREK, *On discrete projection methods for the incompressible Navier–Stokes equations: an algorithmal approach*, Comp. Methods Appl. Mech. Engrg., 143 (1997), pp. 271–288.